



# International Journal for Innovative Engineering and Management Research

A Peer Reviewed Open Access International Journal

www.ijiemr.org

## COPY RIGHT

**2017 IJIEMR.** Personal use of this material is permitted. Permission from IJIEMR must be obtained for all other uses, in any current or future media, including reprinting/republishing this material for advertising or promotional purposes, creating new collective works, for resale or redistribution to servers or lists, or reuse of any copyrighted component of this work in other works. No Reprint should be done to this paper, all copy right is authenticated to Paper Authors

IJIEMR Transactions, online available on 9<sup>th</sup> November 2017. Link :

<http://www.ijiemr.org/downloads.php?vol=Volume-6&issue=ISSUE-10>

Title: Hysteresis Current Control Based Zeta Converter for BLDC Motor Driven Water Pumping System.

Volume 06, Issue 06, Page No: 181 – 190.

Paper Authors

\* **GAYATRI PINGALI, D. PRASAD RAO.**

\* Dept of EEE, Ellenki College of Engineering & Technology.



USE THIS BARCODE TO ACCESS YOUR ONLINE PAPER

To Secure Your Paper As Per **UGC Guidelines** We Are Providing A Electronic Bar Code

## HYSTERESIS CURRENT CONTROL BASED ZETA CONVERTER FOR BLDC MOTOR DRIVEN WATER PUMPING SYSTEM

\*GAYATRI PINGALI, \*\*D. PRASAD RAO

\*PG Scholar, Dept of EEE, Ellenki College of Engineering & Technology, Patalguda; Sangareddy (Dt); Telangana, India.

\*\*Assistant Professor, Dept of EEE, Ellenki College of Engineering & Technology, Patalguda; Sangareddy (Dt); Telangana, India.

[pingali.gayathri@gmail.com](mailto:pingali.gayathri@gmail.com)    [prasad.dama@gmail.com](mailto:prasad.dama@gmail.com)

### ABSTRACT:

In this project fuzzy controlled zeta converter-fed brushless direct current (BLDC) motor drive as a cost-effective solution for low-power applications is presented. The VSI, converting dc output from a zeta converter into ac, feeds the BLDC motor to drive a water pump coupled to its shaft. The VSI is operated in fundamental frequency switching through an electronic commutation of BLDC motor assisted by its built-in encoder. The high frequency switching losses are thereby eliminated, contributing in an increased efficiency of proposed water pumping system. By adjusting the dc link voltage of the voltage source inverter (VSI) feeding a BLDC motor, the speed of the BLDC motor is controlled. This paper deals with the implementation of pulse width modulated Zeta converter, lower total harmonic distortion factor and better efficiency. The proposed zeta converter based BLDC Motor drive is implemented to improve the efficiency of water pumping system and to obtain a wide range of speed control. The system performance can be evaluated. In extension Fuzzy controller is used for better speed response By using MATLAB/SIMULINK software.

**Index Terms**—Brushless dc (BLDC) motor, incremental conductance maximum power point tracking (INC-MPPT), solar photovoltaic (SPV) array, voltage-source inverter (VSI), water pump, zeta converter

### I INTRODUCTION

The drastic reduction in the cost of power electronic devices and annihilation of fossil fuels in near future invite to use the solar photovoltaic (SPV) generated electrical energy for various applications as far as possible. The water pumping, a standalone application of the SPV array-generated electricity, is receiving wide attention nowadays for irrigation in the fields, household applications, and industrial use. Although several researches have been carried out in an area of SPV array-fed water pumping, combining various dc–dc converters and motor drives, the zeta converter in association with a permanent-magnet brushless

dc (BLDC) motor is not explored precisely so far to develop such kind of system. However, the zeta converter has been used in some other SPV-based applications [1]–[3]. Moreover, a topology of SPV array-fed BLDC motor-driven water pump with zeta converter has been reported and its significance has been presented more or less in [4].

Nonetheless, an experimental validation is missing and the absence of extensive literature review and comparison with the existing topologies has concealed the technical contribution and originality of the reported work. The merits of both BLDC motor and zeta converter can contribute to develop an SPV

array-fed water pumping system possessing a potential of operating satisfactorily under dynamically changing atmospheric conditions. The BLDC motor has high reliability, high efficiency, high torque/inertia ratio, improved cooling, low radio frequency interference, and noise and requires practically no maintenance. On the other hand, a zeta converter exhibits the following advantages over the conventional buck, boost, buck–boost converters, and Cuk converter when employed in SPV-based applications.

1) Belonging to a family of buck–boost converters, the zeta converter may be operated either to increase or to decrease the output voltage. This property offers a boundless region for maximum power-point tracking (MPPT) of an SPV array [7]. The MPPT can be performed with simple buck [8] and boost [9] converter if MPP occurs within prescribed limits.

2) This property also facilitates the soft starting of BLDC motor unlike a boost converter which habitually steps up the voltage level at its output, not ensuring soft starting.

3) Unlike a classical buck–boost converter [10], the zeta converter has a continuous output current. The output inductor makes the current continuous and ripples free.

4) Although consisting of same number of components as a Cuk converter [11], the zeta converter operates as non-inverting buck–boost converter unlike an inverting buck–boost and Cuk converter. This property obviates a requirement of associated circuits for negative voltage sensing, and hence reduces the complexity and probability of slow down the system response [12].

These merits of the zeta converter are favorable for proposed SPV array-fed water pumping system. An incremental conductance maximum power point tracking (INC-MPPT) algorithm [8], is used to operate the zeta converter such that SPV array always operates at its MPP. The existing literature exploring SPV array-based BLDC motor-driven water

pump [19] is based on a configuration shown in Fig.1. A dc–dc converter is used for MPPT of an SPV array as usual. Two phase currents are sensed along with Hall signals feedback for control of BLDC motor, resulting in an increased cost. The additional control scheme causes increased cost and complexity, which is required to control the speed of BLDC motor. Moreover, usually a voltage-source inverter (VSI) is operated with high-frequency PWM pulses, resulting in an increased switching loss and hence the reduced efficiency.

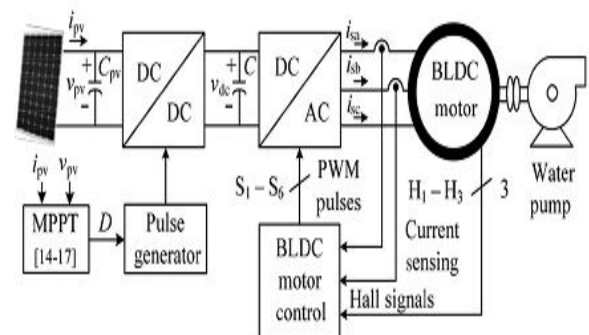


Fig.1. Conventional SPV-fed BLDC motor-driven water pumping system

Although a Z-source inverter (ZSI) replaces dc–dc converter in [22], other schematic of Fig.1 remains unchanged, promising high efficiency and low cost. Contrary to it, ZSI also necessitates phase current and dc link voltage sensing resulting in the complex control and increased cost.

To overcome these problems and drawbacks, a simple, cost effective, and efficient water pumping system based on SPV array-fed BLDC motor is proposed, by modifying the existing topology (Fig. 1) as shown in Fig.2. A zeta converter is utilized to extract the maximum power available from an SPV array, soft starting, and speed control of BLDC motor coupled to a water pump. Due to a single switch, this converter has very good efficiency and offers boundless region for MPPT. This converter is operated in continuous conduction mode (CCM) resulting in a reduced stress on its power devices and components.



Furthermore, the switching loss of VSI is reduced by adopting fundamental frequency switching resulting in an additional power saving and hence an enhanced efficiency. The phase currents as well as the dc link voltage sensors are completely eliminated, offering simple and economical system without sacrificing its performance. The speed of BLDC motor is controlled, without any additional control, through a variable dc link voltage of VSI. Moreover, a soft starting of BLDC motor is achieved by proper initialization of MPPT algorithm of SPV array. These features offer an increased simplicity of proposed system.

The advantages and desirable features of both zeta converter and BLDC motor drive contribute to develop a simple, efficient, cost-effective, and reliable water pumping system based on solar PV energy. Simulation results using MATLAB/Simulink and experimental performances are examined to demonstrate the starting, dynamics, and steady-state behavior of proposed water pumping system subjected to practical operating conditions. The SPV array and BLDC motor are designed such that proposed system always exhibits good performance regardless of solar irradiance level.

## II CONFIGURATION OF PROPOSEDSYSTEM

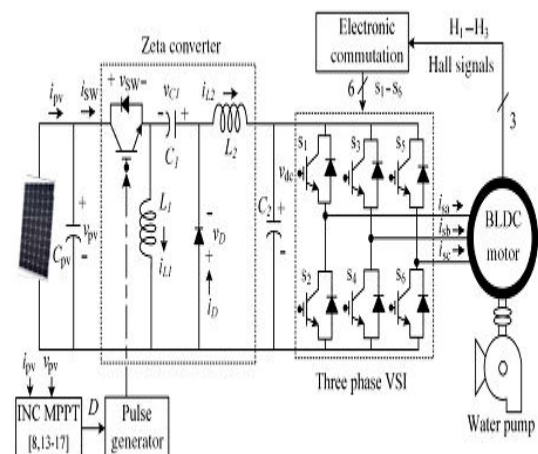
The structure of proposed SPV array-fed BLDC motor driven water pumping system employing a zeta converter is shown in Fig.2. The proposed system consists of (left to right) an SPV array, a zeta converter, a VSI, a BLDC motor, and a water pump. The BLDC motor has an inbuilt encoder. The pulse generator is used to operate the zeta converter. A step-by-step operation of proposed system is elaborated in Section 3.3 in detail.

## III OPERATION OF PROPOSEDSYSTEM

The SPV array generates the electrical power demanded by the motor-pump. This

electrical power is fed to the motor pump via a zeta converter and a VSI. The SPV array appears as a power source for the zeta converter as shown in Fig.3.2. Ideally, the same amount of power is transferred at the output of zeta converter which appears as an input source for the VSI. In practice, due to the various losses associated with a dc– dc converter [23], slightly less amount of power is transferred to feed the VSI. The pulse generator generates, through INCMPPPT algorithm, switching pulses for insulated gate bipolar transistor (IGBT) switch of the zeta converter. The INC-MPPT algorithm uses voltage and current as feedback from SPV array and generates an optimum value of duty cycle. Further, it generates actual switching pulse by comparing the duty cycle with a high-frequency carrier wave. In this way, the maximum power extraction and hence the efficiency optimization of the SPV array is accomplished.

The VSI, converting dc output from a zeta converter into ac, feeds the BLDC motor to drive a water pump coupled to its shaft. The VSI is operated in fundamental frequency switching through an electronic commutation of BLDC motor assisted by its built-in encoder. The high frequency switching losses are thereby eliminated, contributing in an increased efficiency of proposed water pumping system.



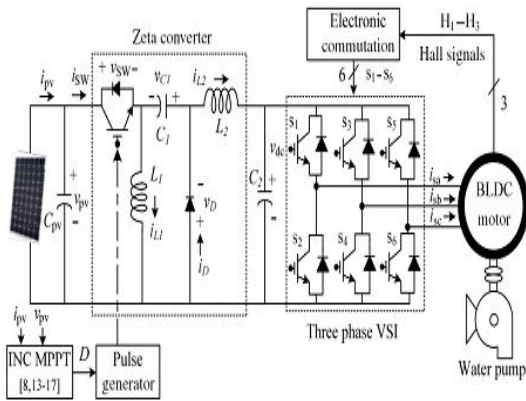


Fig.2. Proposed SPV-zeta converter-fed BLDC motor drive for water pump

## IV DESIGN OF PROPOSED SYSTEM

Various operating stages shown in Fig.2 are properly designed to develop an effective water pumping system, capable of operating under uncertain conditions. A BLDC motor of 2.89-kW power rating and an SPV array of 3.4-kW peak power capacity under standard test conditions (STC) are selected to design the proposed system. The detailed designs of various stages such as SPV array, zeta converter, and water pump are described as follows.

### 1 Design of SPV Array

As per above discussion, the practical converters are associated with various power losses. In addition, the performance of BLDC motor-pump is influenced by associated mechanical and electrical losses. To compensate these losses, the size of SPV array is selected with slightly more peak power capacity to ensure the satisfactory operation regardless of power losses. Therefore, the SPV array of peak power capacity of  $P_{mpp}=3.4$  kW under STC (STC:  $1000 \text{ W/m}^2$ ,  $25^\circ\text{C}$ , AM 1.5), slightly more than demanded by the motor-pump is selected and its parameters are designed accordingly. Solar World make Sun module Plus SW 280 mono [24] SPV module is selected to design the SPV array of an appropriate size. Electrical specifications of

this module are listed in Table 1 and numbers of modules required to connect in series/parallel are estimated by selecting the voltage of SPV array at MPP under STC as  $V_{mpp}=187.2\text{V}$ .

TABLE 1

Specifications of Sun module plus SW 280 mono SPV Module

|   |      |
|---|------|
| Peak power, $P_m$ (W)                         | 280  |
| Open circuit voltage, $V_o$ (V)               | 39.5 |
| Voltage at MPP, $V_m$ (V)                     | 31.2 |
| Short circuit current, $I_s$ (A)              | 9.71 |
| Current at MPP, $I_m$ (A)                     | 9.07 |
| Number of cells connected in series, $N_{ss}$ | 60   |

The current of SPV array at MPP  $I_{mpp}$  is estimated as

$$I_{mpp} = P_{mpp}/V_{mpp} = 3400/187.2 = 18.16 \quad (1)$$

The numbers of modules required to connect in series are as follows:

$$N_s = V_{mpp}/V_m = 187.2/31.2 = 6 \quad (2)$$

The numbers of modules required to connect in parallel are as follows:

$$N_p = I_{mpp}/I_m = 18.16/9.07 = 2 \quad (3)$$

Connecting six modules in series, having two strings in parallel, an SPV array of required size is designed for the proposed system.

### 2 Design of Zeta Converter

The zeta converter is the next stage to the SPV array. Its design consists of an estimation of various components such as input inductor  $L_1$ , output inductor  $L_2$ , and intermediate capacitor  $C_1$ . These components are designed such that the zeta converter always operates in CCM resulting in reduced stress on its components and devices. An estimation of the duty cycle  $D$  initiates the design of zeta converter which is estimated as [6]

$$D = \frac{V_{dc}}{V_{dc} + V_{mpp}} = \frac{200}{200 + 187.2} = 0.52 \quad (4)$$

Where  $V_{dc}$  is an average value of output voltage of the zeta converter (dc link voltage of VSI) equal to the dc voltage rating of the BLDC motor.

An average current flowing through the dc link of the VSI  $I_{dc}$  is estimated as

$$I_{dc} = P_{mpp}/V_{dc} = 3400/200 = 17 \text{ A.} \quad (5)$$

Then,  $L_1$ ,  $L_2$ , and  $C_1$  are estimated as

$$L_1 = \frac{DV_{mpp}}{f_{sw}\Delta I_{L1}} = \frac{0.52 \times 187.2}{20000 \times 18.16 \times 0.06} = 4.5 \times 10^{-3} \approx 5 \text{ mH} \quad (6)$$

$$L_2 = \frac{(1-D)V_{dc}}{f_{sw}\Delta I_{L2}} = \frac{(1-0.52) \times 200}{20000 \times 17 \times 0.06} = 4.7 \times 10^{-3} \approx 5 \text{ mH} \quad (7)$$

$$C_1 = \frac{DI_{dc}}{f_{sw}\Delta V_{C1}} = \frac{0.52 \times 17}{20000 \times 200 \times 0.1} = 22 \text{ }\mu\text{F} \quad (8)$$

Where  $f_{sw}$  is the switching frequency of IGBT switch of the zeta converter;  $\Delta I_{L1}$  is the amount of permitted ripple in the current flowing through  $L_1$ , same as  $I_{L1}=I_{mpp}$ ;  $\Delta I_{L2}$  is the amount of permitted ripple in the current flowing through  $L_2$ , same as  $I_{L2}=I_{dc}$ ;  $\Delta V_{C1}$  is permitted ripple in the voltage across  $C_1$ , same as  $V_{C1}=V_{dc}$ .

### 3 Estimation of DC-Link Capacitor of VSI

A new design approach for estimation of dc-link capacitor of the VSI is presented here. This approach is based on a fact that sixth harmonic component of the supply (ac) voltage is reflected on the dc side as a dominant harmonic in the three-phase supply system [25]. Here, the fundamental frequencies of output voltage of the VSI are estimated corresponding to the rated speed and the minimum speed of BLDC motor essentially

required pumping the water. These two frequencies are further used to estimate the values of their corresponding capacitors. Out of these two estimated capacitors, larger one is selected to assure a satisfactory operation of proposed system even under the minimum solar irradiance level.

The fundamental output frequency of VSI corresponding to the rated speed of BLDC motor  $\omega_{rated}$  is estimated as

$$\omega_{rated} = 2\pi f_{rated} = 2\pi \frac{N_{rated}P}{120} = 2\pi \times \frac{3000 \times 6}{120} = 942 \text{ rad/s.} \quad (9)$$

The fundamental output frequency of the VSI corresponding to the minimum speed of the BLDC motor essentially required to pump the water ( $N=1100$  r/min)  $\omega_{min}$  is estimated as

$$\omega_{min} = 2\pi f_{min} = 2\pi \frac{NP}{120} = 2\pi \times \frac{1100 \times 6}{120} = 345.57 \text{ rad/s} \quad (10)$$

Where  $f_{rated}$  and  $f_{min}$  are fundamental frequencies of output voltage of VSI corresponding to a rated speed and a minimum speed of BLDC motor essentially required to pump the water, respectively, in Hz;  $N_{rated}$  is rated speed of the BLDC motor;  $P$  is a number of poles in the BLDC motor.

The value of dc link capacitor of VSI at  $\omega_{rated}$  is as follows:

$$C_{2,rated} = \frac{I_{dc}}{6 \times \omega_{rated} \times \Delta V_{dc}} = \frac{17}{6 \times 942 \times 200 \times 0.1} = 150.4 \text{ }\mu\text{F.} \quad (11)$$

Similarly, a value of dc link capacitor of VSI at  $\omega_{min}$  is as follows:

$$C_{2,min} = \frac{I_{dc}}{6 \times \omega_{min} \times \Delta V_{dc}} = \frac{17}{6 \times 345.57 \times 200 \times 0.1} = 410 \text{ }\mu\text{F} \quad (12)$$

Where  $\Delta V_{dc}$  is an amount of permitted ripple in voltage across dc-link capacitor  $C_2$ .



Finally,  $C_2= 410\mu\text{F}$  is selected to design the dc-link capacitor.

#### 4 Design of Water Pump

To estimate the proportionality constant  $K$  for the selected water pump, its power–speed characteristics is used as

$$K = \frac{P}{\omega_r^3} = \frac{2.89 \times 10^3}{(2\pi \times 3000/60)^3} = 9.32 \times 10^{-5} \quad (13)$$

Where  $P=2.89$  kW is rated power developed by the BLDC motor and  $\omega_r$  is rated mechanical speed of the rotor (3000 r/min) in rad/s.

A water pump with these data is selected for proposed system.

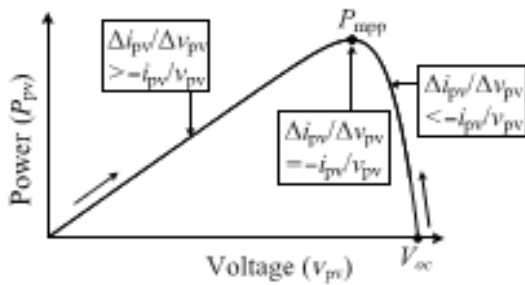


Fig.3. Illustration of INC-MPPT with SPV array  $P_{pv} - v_{pv}$  characteristics.

TABLE 2

Switching States for Electronic Commutation of BLDC Motor

| Rotor position $\theta$ (°) | Hall signals |       |       | Switching states |       |       |       |       |       |
|-----------------------------|--------------|-------|-------|------------------|-------|-------|-------|-------|-------|
|                             | $H_3$        | $H_2$ | $H_1$ | $S_1$            | $S_2$ | $S_3$ | $S_4$ | $S_5$ | $S_6$ |
| NA                          | 0            | 0     | 0     | 0                | 0     | 0     | 0     | 0     | 0     |
| 0-60                        | 1            | 0     | 1     | 1                | 0     | 0     | 1     | 0     | 0     |
| 60-120                      | 0            | 0     | 1     | 1                | 0     | 0     | 0     | 0     | 1     |
| 120-180                     | 0            | 1     | 1     | 0                | 0     | 1     | 0     | 0     | 1     |
| 180-240                     | 0            | 1     | 0     | 0                | 1     | 1     | 0     | 0     | 0     |
| 240-300                     | 1            | 1     | 0     | 0                | 1     | 0     | 0     | 1     | 0     |
| 300-360                     | 1            | 0     | 0     | 0                | 0     | 0     | 1     | 1     | 0     |
| NA                          | 1            | 1     | 1     | 0                | 0     | 0     | 0     | 0     | 0     |

#### V CONTROL OF PROPOSED SYSTEM

The proposed system is controlled in two stages. These two control techniques, viz., MPPT and electronic commutation, are discussed as follows.

#### 1 INC-MPPT Algorithm

An efficient and commonly used INC-MPPT technique [8], [13] in various SPV array based applications is utilized in order to optimize the power available from a SPV array and to facilitate a soft starting of BLDC motor. This technique allows perturbation in either the SPV array voltage or the duty cycle. The former calls for a proportional-integral (PI) controller to generate a duty cycle [8] for the zeta converter, which increases the complexity. Hence, the direct duty cycle control is adapted in this work. The INC-MPPT algorithm determines the direction of perturbation based on the slope of  $P_{pv}-v_{pv}$  curve, shown in Fig.3. As shown in Fig.3, the slope is zero at MPP, positive on the left, and negative on the right of MPP, i.e.,

$$\left. \begin{aligned} \frac{dP_{pv}}{dv_{pv}} &= 0; && \text{at mpp} \\ \frac{dP_{pv}}{dv_{pv}} &> 0; && \text{left of mpp} \\ \frac{dP_{pv}}{dv_{pv}} &< 0; && \text{right of mpp} \end{aligned} \right\} \quad (14)$$

Since

$$\frac{dP_{pv}}{dv_{pv}} = \frac{d(v_{pv} * i_{pv})}{dv_{pv}} = i_{pv} + v_{pv} * \frac{di_{pv}}{dv_{pv}} \approx i_{pv} + v_{pv} * \frac{\Delta i_{pv}}{\Delta v_{pv}} \quad (15)$$

Therefore, (14) is rewritten as

$$\left. \begin{aligned} \frac{\Delta i_{pv}}{\Delta v_{pv}} &= -\frac{i_{pv}}{v_{pv}}; && \text{at mpp} \\ \frac{\Delta i_{pv}}{\Delta v_{pv}} &> -\frac{i_{pv}}{v_{pv}}; && \text{left of mpp} \\ \frac{\Delta i_{pv}}{\Delta v_{pv}} &< -\frac{i_{pv}}{v_{pv}}; && \text{right of mpp} \end{aligned} \right\} \quad (16)$$

Thus, based on the relation between INC and instantaneous conductance, the

controller decides the direction of perturbation as shown in Fig. 3, and increases/decreases the duty cycle accordingly. For instance, on the right of MPP, the duty cycle is increased with a fixed perturbation size until the direction reverses. Ideally, the perturbation stops once the operating point reaches the MPP. However, in practice, operating point oscillates around the MPP.

As the perturbation size reduces, the controller takes more time to track the MPP of SPV array. An intellectual agreement between the tracking time and the perturbation size is held to fulfill the objectives of MPPT and soft starting of BLDC motor. In order to achieve soft starting, the initial value of duty cycle is set as zero. In addition, an optimum value of perturbation size ( $\Delta D=0.001$ ) is selected, which contributes to soft starting and also minimizes oscillations around the MPP.

## 2 Electronic Commutation of BLDC Motor

The BLDC motor is controlled using a VSI operated through an electronic commutation of BLDC motor. An electronic commutation of BLDC motor stands for commutating the currents flowing through its windings in a predefined sequence using decoder logic. It symmetrically places the dc input current at the center of each phase voltage for  $120^\circ$ . Six switching pulses are generated as per the various possible combinations of three Hall-effect signals. These three Hall-effect signals are produced by an inbuilt encoder according to the rotor position.

A particular combination of Hall-effect signals is produced for each specific range of rotor position at an interval of  $60^\circ$ . The generation of six switching states with the estimation of rotor position is tabularized in Table II. It is perceptible that only two switches conduct at a time, resulting in  $120^\circ$  conduction mode of operation of VSI and hence the reduced conduction losses. Besides this, the electronic commutation provides fundamental frequency switching of the VSI; hence, losses

associated with high-frequency PWM switching are eliminated. A motor power company makes BLDC motor [28] with inbuilt encoder is selected for proposed system and its detailed specifications are given in the Appendixes.

## VI HYSTERESIS CONTROLLER

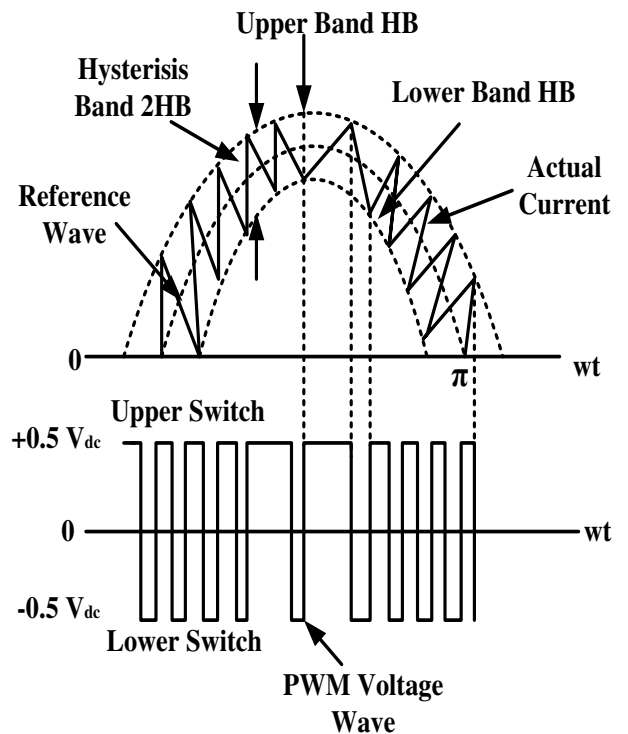


Fig.4. Basic principal of hysteresis controller

With the hysteresis control, limit bands are set on either side of a signal representing the desired output waveform [6]. The inverter switches are operated as the generated signals within limits. The control circuit generates the sine reference signal wave of desired magnitude and frequency, and it is compared with the actual signal. As the signal exceeds a prescribed hysteresis band, the upper switch in the half bridge is turned OFF and the lower switch is turned ON. As the signal crosses the lower limit, the lower switch is turned OFF and the upper switch is turned ON. The actual signal wave is thus forced to track the sine



reference wave within the hysteresis band limits.

### Pulse Generation Technique

Pulse generation is main and important part of this technique. Here we have used hysteresis technique for switching technique.

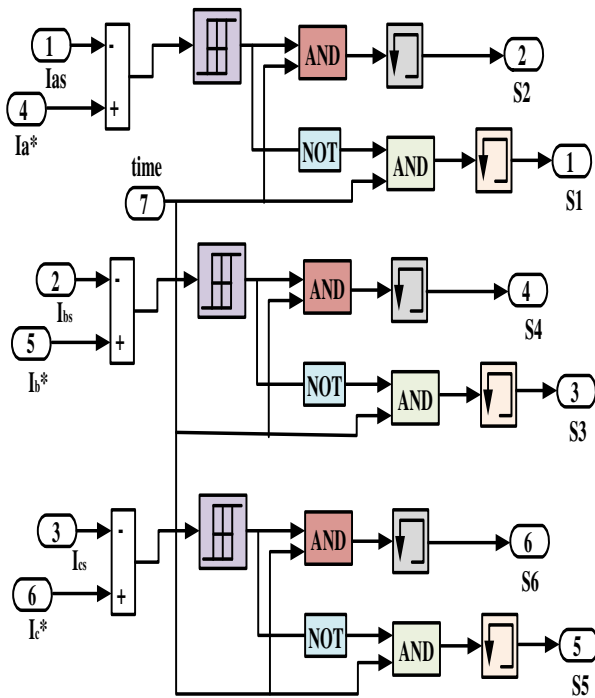


FIG.5. PULSE GENERATION DIAGRAM

## VII .MATLAB/SIMULATION RESULTS

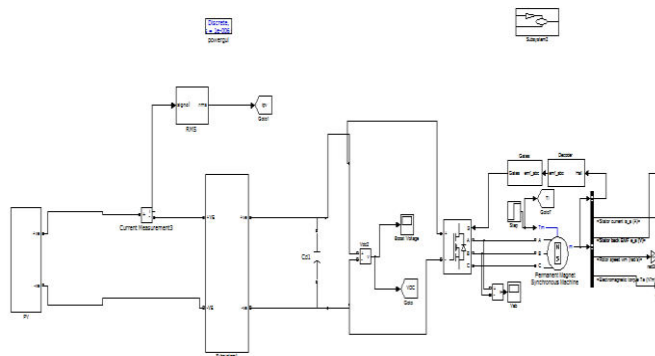
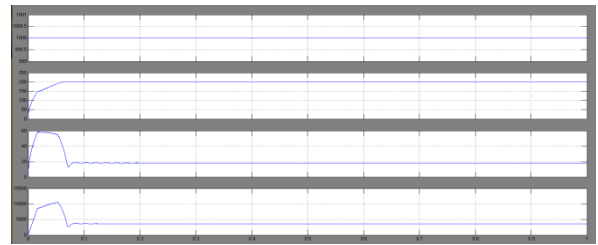
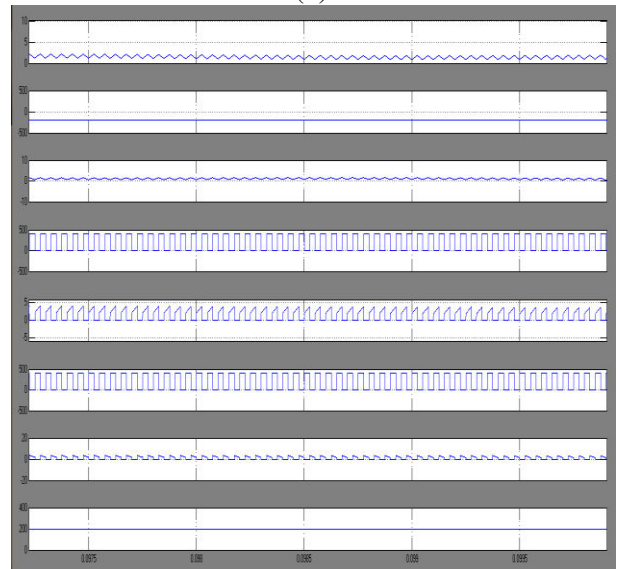


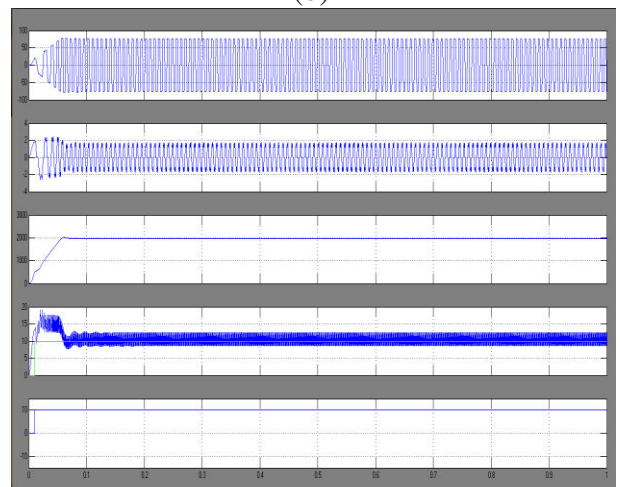
Fig 6 simulation circuit Conventional SPV-fed BLDC motor-driven water pumping system



(a)



(b)



(c)

Fig 7 Starting and steady-state performances of the proposed SPV arraybased zeta converter-fed BLDC motor drive for water pump. (a) SPV array variables. (b) Zeta converter variables. (c) BLDC motor-pump variables

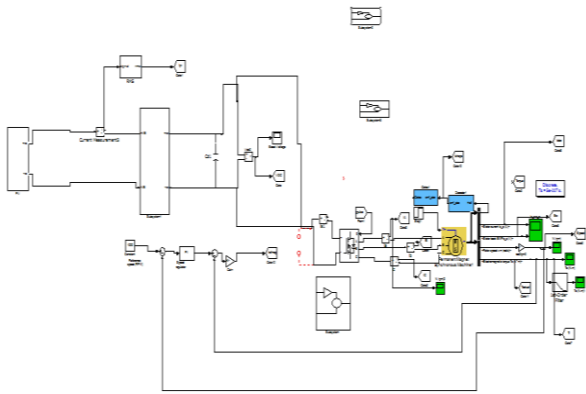


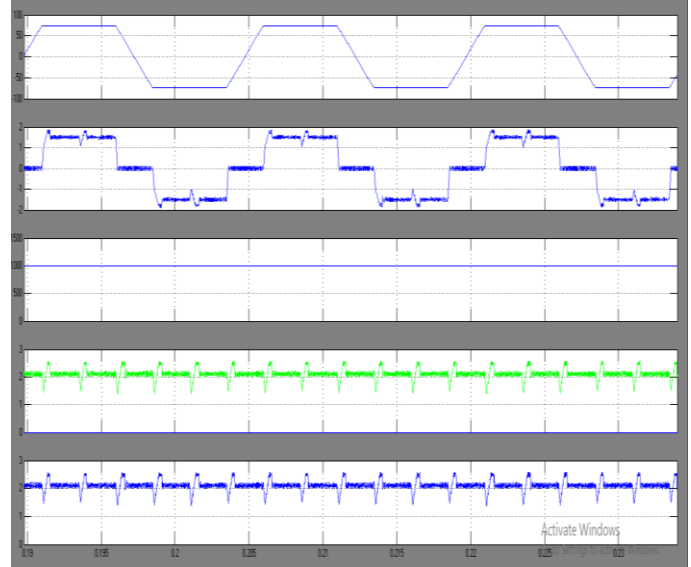
Fig 8 simulation circuit Conventional SPV-fed BLDC motor-driven water pumping system with speed controller



(a)



(b)



(c)

Fig 9 Starting and steady-state performances of the proposed SPV arraybased zeta converter-fed BLDC motor drive for water pump. (a) SPV array variables. (b) Zeta converter variables. (c) BLDC motor-pump variables with hysteresis voltage controller

## CONCLUSION

The SPV array-zeta converter-fed VSI-BLDC motor-pump has been proposed and its suitability has been demonstrated through simulated results and experimental validation. The proposed system has been designed and modeled appropriately to accomplish the desired objectives and validated to examine various performances under starting, dynamic, and steady-state conditions. The performance evaluation has justified the combination of zeta converter and BLDC motor for SPV array-based water pumping. The system under study has shown various desired functions such as maximum power extraction of the SPV array, soft starting of BLDC motor, fundamental frequency switching of VSI resulting in a reduced switching losses, speed control of BLDC motor without any additional control, and an elimination of phase current and dc-link voltage sensing, resulting in the reduced cost and complexity. The proposed system has

operated with hysteresis voltage controller successfully even under minimum solar irradiance.

## REFERENCES

- [1] M. Uno and A. Kukita, "Single-switch voltage equalizer using multi stacked buck–boost converters for partially-shaded photovoltaic modules," *IEEE Trans. Power Electron.*, vol. 30, no. 6, pp. 3091–3105, Jun. 2015.
- [2] R. Arulmurugan and N. Suthanthiravanitha, "Model and design of a fuzzy-based Hopfield NN tracking controller for standalone PV applications," *Elect. Power Syst. Res.*, vol. 120, pp. 184–193, Mar. 2015.
- [3] S. Satapathy, K. M. Dash, and B. C. Babu, "Variable step size MPPT algorithm for photo voltaic array using zeta converter—A comparative analysis," in *Proc. Students Conf. Eng. Syst. (SCES)*, Apr. 12–14, 2013, pp. 1–6.
- [4] R. Kumar and B. Singh, "BLDC motor driven solar PV array fed water pumping system employing zeta converter," in *Proc. 6th IEEE India Int. Conf. Power Electron. (IICPE)*, Dec. 8–10, 2014, pp. 1–6.
- [5] B. Singh, V. Bist, A. Chandra, and K. Al-Haddad, "Power factor correction in bridgeless-Luo converter-fed BLDC motor drive," *IEEE Trans. Ind. Appl.*, vol. 51, no. 2, pp. 1179–1188, Mar./Apr. 2015.
- [6] B. Singh and V. Bist, "Power quality improvements in a zeta converter for brushless dc motor drives," *IET Sci. Meas. Technol.*, vol. 9, no. 3, pp. 351–361, May 2015.
- [7] R. F. Coelho, W. M. dos Santos, and D. C. Martins, "Influence of power converters on PV maximum power point tracking efficiency," in *Proc. 10th IEEE/IAS Int. Conf. Ind. Appl. (INDUSCON)*, Nov. 5–7, 2012, pp. 1–8.
- [8] M. A. Elgendy, B. Zahawi, and D. J. Atkinson, "Assessment of the incremental conductance maximum power point tracking algorithm," *IEEE Trans. Sustain. Energy*, vol. 4, no. 1, pp. 108–117, Jan. 2013.
- [9] M. Sitbon, S. Schacham, and A. Kuperman, "Disturbance observer based voltage regulation of current-mode-boost-converter-interfaced photovoltaic generator," *IEEE Trans. Ind. Electron.*, vol. 62, no. 9, pp. 5776–5785, Sep. 2015.
- [10] R. Kumar and B. Singh, "Buck–boost converter fed BLDC motor drive for solar PV array based water pumping," in *Proc. IEEE Int. Conf. Power Electron. Drives Energy Syst. (PEDES)*, Dec. 16–19, 2014, pp. 1–6.
- [11] A. H. El Khateb, N. Abd. Rahim, J. Selvaraj, and B. W. Williams, "DC to-dc converter with low input current ripple for maximum photovoltaic power extraction," *IEEE Trans. Ind. Electron.*, vol. 62, no. 4, pp. 2246–2256, Apr. 2015.
- [12] D. D. C. Lu and Q. N. Nguyen, "A photovoltaic panel emulator using a buck–boost dc/dc converter and a low cost micro-controller," *Solar Energy*, vol. 86, no. 5, pp. 1477–1484, May 2012.
- [13] Z. Xuesong, S. Daichun, M. Youjie, and C. Deshu, "The simulation and design for MPPT of PV system based on incremental conductance method," in *Proc. WASE Int. Conf. Inf. Eng. (ICIE)*, Aug. 14–15, 2010, vol. 2, pp. 314–317.
- [14] A. R. Reisi, M. H. Moradi, and S. Jamasb, "Classification and comparison of maximum power point tracking techniques for photovoltaic system: A review," *Renew. Sustain. Energy Rev.*, vol. 19, pp. 433–443, Mar. 2013.
- [15] B. Bendib, H. Belmili, and F. Krim, "A survey of the most used MPPT methods: Conventional and advanced algorithms applied for photovoltaic systems," *Renew. Sustain. Energy Rev.*, vol. 45, pp. 637–648, May 2015.
- [16] B. Subudhi and R. Pradhan, "A comparative study on maximum power point tracking techniques for photovoltaic power systems," *IEEE Trans. Sustain. Energy*, vol. 4, no. 1, pp. 89–98, Jan. 2013.